Characterization of near-terahertz complementary metal-oxide semiconductor circuits using a Fourier-transform interferometer

D. J. Arenas,[1] Dongha Shim,[2] D. I. Koukis,[3] Eunyoung Seok,[2,4]
D. B. Tanner,[3] and Kenneth K. O[5]
[1]*Department of Physics, University of North Florida, Jacksonville, Florida 32254, USA*
[2]*Department of Electrical and Computer Engineering, University of Florida, Gainesville, Florida 32611, USA*
[3]*Department of Physics, University of Florida, Gainesville, Florida 32611, USA*
[4]*Texas Instruments, Inc., Dallas, Texas 75266, USA*
[5]*Texas Analog Center of Excellence & Department of Electrical Engineering, University of Texas, Dallas, Texas 75080, USA*

(Received 18 May 2011; accepted 13 September 2011; published online 24 October 2011)

Optical methods for measuring of the emission spectra of oscillator circuits operating in the 400–600 GHz range are described. The emitted power from patch antennas included in the circuits is measured by placing the circuit in the source chamber of a Fourier-transform interferometric spectrometer. The results show that this optical technique is useful for measuring circuits pushing the frontier in operating frequency. The technique also allows the characterization of the circuit by measuring the power radiated in the fundamental and in the harmonics. This capability is useful for oscillator architectures designed to cancel the fundamental and use higher harmonics. The radiated power was measured using two techniques: direct measurement of the power by placing the device in front of a bolometer of known responsivity, and by comparison to the estimated power from blackbody sources. The latter technique showed that these circuits have higher emission than blackbody sources at the operating frequencies, and, therefore, offer potential spectroscopy applications.
 [doi:10.1063/1.3647223]

I. INTRODUCTION

The terahertz (THz) region of the spectrum is now considered to span the 0.3–3 THz range,[1] although some authors may extend this definition to 30 THz.[2] This region of the spectrum, also called the far infrared or millimeter-wave regime, has attracted attention from many fields. In bio-imaging, THz radiation is desirable because (in contrast to x-rays) it can penetrate organic materials without ionization. Also, THz radiation is absorbed by water, allowing the study of differing water contents in cells[3] and, hence, the detection of certain cancer cells.[4,5] The high transmission of THz radiation through non-metallic media, such as shoes, clothes, and cardboard is contrasted by high reflection for metals, motivating the use of THz imaging for detection of concealed weapons.[6,7] Furthermore, there is continuous research in use of THz wavelengths for the detection of dangerous materials, such as explosives,[8,9] chemical agents,[10,11] and illicit drugs.[2,12] In addition to the obvious uses in defense and medical applications, the THz region is also useful for fundamental research. This research includes spectroscopy to study interesting materials, such as multiferroics,[13–16] manganites,[17] graphite/graphene,[18–20] superconductors,[21–24] topological insulators, [25] and others.

The THz region, where optical spectroscopy and circuit technology meet, has been considered to be a poorly developed and difficult region of the spectrum due to the lack of intense sources and sensitive detectors.[26] For spectroscopy, blackbody (thermal) sources have been used to good effect, even though their intensity is weak at these low frequencies, requiring helium-cooled bolometers sensitive enough to measure the available powers, often nW or lower.[21,27,28] For a long time, the frequencies in the THz region were considered too fast for solid-state circuits, and too slow for solid-state lasers.[29] One of the first alternative ways to generate THz radiation began in the sixties with the use of nonlinear crystals for difference-frequency generation,[30] and parametric amplification.[31–34] Another explosion in THz research occurred in the mid eighties with the use of femtosecond lasers to induce THz radiation from various systems; such as photoconducting structures[35–40] and electro-optic materials.[41,42] Femtosecond lasers remain a great tool used in terahertz time-domain spectroscopy,[1,43] which uses photoconductive antennas [44,45] and electro-optic materials as detectors.[46,47] For continuous-wave (c.w.) operation in the THz region, quantum-cascade lasers have been an important focus in the last decade.[48–51] The efforts have produced high power c.w. lasers at low frequencies,[52] and increases in operating temperature.[53,54] For the last few decades, new exciting and powerful sources have appeared, including free electron lasers,[29] synchrotrons,[55,56] and other systems which use relativistic electrons to generate THz radiation.[57–59]

These new THz sources are big and their costs are high. In the future, some applications will require more compact, and, more importantly, lower-cost sources. The low-cost requirement will also apply to THz detectors. Here, we consider mainstream silicon technology, such as complementary metal-oxide semiconductor (CMOS) circuits. The first objective for this technology is to design and build faster circuits, heading towards THz operating frequencies.[60] Therefore, the effort to build cost-efficient THz sources and detectors can be directly based on the extensive research towards faster circuits

for the computer industry. Previously, we reported a 410 GHz CMOS circuit, which at the time of publication had the highest operating frequency of any semiconductor technology.[61] Later on, we reported a 590 GHz circuit using a 0.12 μm SiGE BiCMOS process.[62] Because these circuits operate at higher frequencies than other electronic circuits, there are no electronic probes to measure accurately their operating frequency. In our previous publications,[61,62] we demonstrated that a Fourier-transform infrared spectrometer (FTIR) can be used to measure the operating frequency of these circuits. This paper has three main purposes. One purpose is to show in detail the use of the FTIR system for circuit characterization. Second, we show that the power emitted from the circuits can be estimated in the FTIR system by comparison to blackbody sources. And third, we report that the power from the recently-built near-THz circuits is higher than the circuits reported earlier. They also have higher power at the emitted frequencies compared to commonly used blackbody sources. The brightness (emission per unit area) is $\sim 10^4$ higher for the circuits than that for the blackbody sources. The higher power offers potential spectroscopy applications.

II. EXPERIMENTAL PROCEDURES

A. Circuit design

The 410 GHz circuit uses a push-push oscillator architecture to extract the second harmonic of a 205 GHz oscillator circuit. Figure 1 shows a diagram of this circuit. The oscillator is equipped with a patch antenna to extract the signal. The resonant frequency of the circuit is determined by the capacitances of the transistors M_1 and M_2 and the inductances of L_1 and L_2. In the oscillator, the unity gain frequency of the amplifier (i.e., transistor) limits the maximum frequency of the fundamental. For our circuits, this frequency is around 200 GHz. To increase the operating frequency, the second harmonic of the fundamental was generated by using a push-push oscillator architecture. The cross-coupled design of the transistors in the oscillator core is such that their signals are 180° out of phase. The nonlinearity of each transistor generates a second harmonic signal, which, unlike the fundamental, adds in phase at the output. This can be shown by writing an expression for the currents at transistors 1 and 2 (J_{M1} and J_{M2}),

$$J_{M1} = \sigma^{(1)} E e^{i\omega t} + \sigma^{(2)} (E e^{i\omega t})^2 + \ldots, \quad (1)$$

$$J_{M2} = \sigma^{(1)} E e^{i\omega t} e^{i\pi} + \sigma^{(2)} (E e^{i\omega t} e^{i\pi})^2 + \ldots, \quad (2)$$

where $\sigma^{(1)}$ is the linear conductivity of the transistors (assumed the same for both), and $\sigma^{(2)}$ is the second order nonlinear term. At the output node, the fundamental signals are attenuated due to their phase difference, $e^{i\pi}$, while the out-of-phase term disappears for the second harmonic:

$$J_{M1} + J_{M2} = 2\sigma^{(2)} E^2 e^{i2\omega t}. \quad (3)$$

Two PMOS transistors (M_3 and M_4) are used to bias the core, and two quarter-wave transmission lines ($T.L_1$ and $T.L_2$) are used to isolate these components from the fundamental and second harmonic. More details on the circuit and patch antenna design can be found in Refs. 61–63.

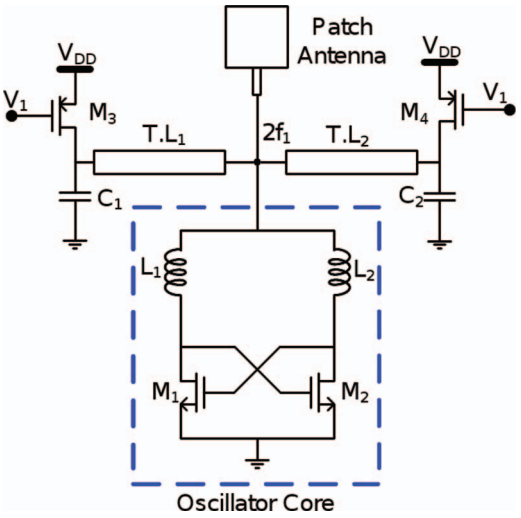

FIG. 1. (Color online) The 410 GHz oscillator. Circuit diagram for the push-push oscillator system with an on-chip patch antenna. This circuit extracts the second harmonic from a 205 GHz fundamental. This circuit had the highest operating frequency of any semiconductor technology in 2008. Further details of the design and manufacture can be found in the work by Seok *et al.* (See Ref. 61.)

Figure 2 shows the Colpitts oscillator architecture for the 590 GHz circuit. This circuit is designed to extract the fourth harmonic signal. Details of the design and manufacture of this circuit can be found in the work by Seok *et al.*[62] At this point, we want to emphasize that these circuits are designed to extract the signal at a chosen harmonic; therefore, to

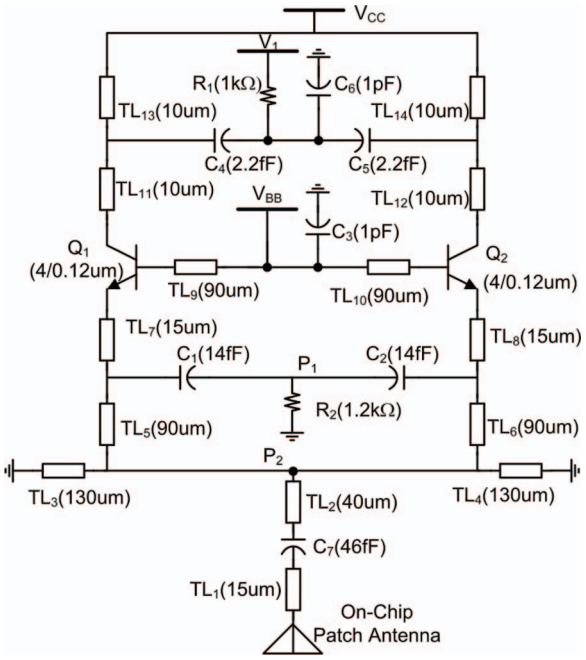

FIG. 2. The 590 GHz oscillator. Schematic of an antenna-loaded oscillator operating in quadruple order. The circuit is designed to produce the fourth harmonic signal of a 200 GHz fundamental. Reprinted with permission from E. Seok *et al.*, *Generation of Second and Fourth Harmonic Signals Using a Balanced Colpitts Oscillator With a Patch Antenna*, IEEE Microwave and Wireless Components Letters **20**, 554 (2010). © IEEE 2010.

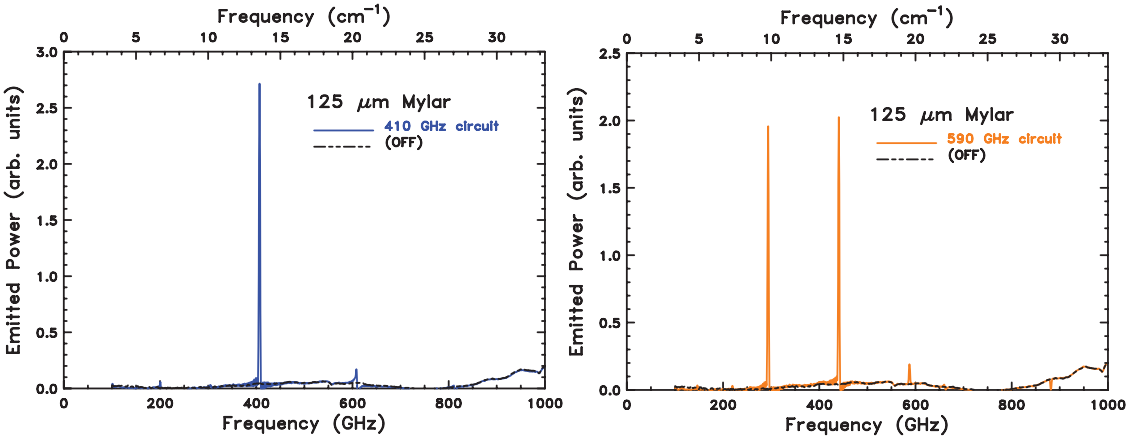

FIG. 3. (Color online) Emission spectrum of the THz circuits. Frequencies shown in GHz and in cm^{-1}. (1 cm^{-1} = 30 GHz). The emission spectra were measured with the Mylar 125 μm beamsplitter. The left figure shows the emission spectrum of the 410 GHz circuit ON and OFF. The 410 GHz emission line corresponds to the second harmonic of the fundamental. The right figure shows the 590 GHz circuit. The 590 GHz line from this circuit corresponds to the fourth harmonic of the fundamental. The emission spectrum shows that the emission of the second and third harmonic is very strong.

characterize these circuits, it is useful to see if the circuit works at the chosen harmonic, and that the fundamental and any other undesired harmonics are canceled. As we will discuss below, FTIR has proven useful for this purpose.

B. Detection of the radiation using an interferometer

The operating-frequency of the circuits was measured using the radiation from their patch antennas.[61,62] The radiation was measured using a Bruker 113v FTIR system. The basic components of the Bruker 113v are the source, an interferometer, and a detector. Widely used sources for the Bruker 113v include globar (silicon carbide), tungsten resistive lamps, and mercury-arc lamps. The radiation power of these blackbody sources was used as a reference by placing the circuits in the mercury-arc source housing. The interferometer used 23 and 125 μm (0.9 and 5 mil) Mylar beamsplitters. The 125 μm (5 mil) thickness of the beamsplitter was chosen to increase the sensitivity around 400–600 GHz. A 23 μm (0.9 mil) thick beamsplitter was also used to confirm the results. This thickness is commonly used in spectroscopy for the 20–100 cm^{-1} region (0.6–3 THz). The scanning speed of the interferometer was varied to diagnose 60 Hz (and harmonics) pickup, since the computed infrared frequency of these peaks changes when the scanning velocity is varied. The procedure showed that the peaks due to the 60 Hz noise and its harmonics were negligible. The resolution of our measurements was 0.1 cm^{-1} (3 GHz), which is the limit set by path length difference (10 cm) of the interferometer. A Norton-Beer apodization function was used in the analysis of the interferogram, and the Mertz function was used for phase correction. For the detector, we used a 4.2 K cooled Si bolometer from Infrared Laboratories and checked our results using two different examples (HD-3, serials 1378 and 1730).

To estimate the absolute power emitted from the antenna, the source and the detector were removed from the interferometer, and the source was placed directly at the input of the bolometer. The signal to noise ratio was greatly improved by modulating the circuit at 100 Hz and using a lock-in amplifier. A lock-in amplifier takes a signal modulated in frequency $S(\omega)$ and a reference $\sin(\omega_r t - \phi)$ and amplifies only the amplitude V of the ω_r component by performing the integral:

$$V = \frac{1}{T}\int_0^T S(\omega)\sin(\omega_r t - \phi)dt, \tag{4}$$

where T is an integration time larger than the period of the reference signal as well as the period of other components in $S(\omega)$. Other frequencies are filtered due to the orthogonality of sine and cosine functions. The phase ϕ is adjusted to put reference and signal in phase. If we assume a white noise spectrum (this assumption and the length of T can demand the use of low and high pass electronic filters), then the signal/noise ratio is improved by attenuating the noise at frequencies other than ω_r, and keeping only the noise in the bandwidth at the reference frequency. The absolute power radiated from the source was estimated by using the readout from the lock-in setup, and comparing it to the 1.10×10^4 V/W optical responsivity of the bolometer (as reported by Infrared Laboratories). This procedure yields the total power emitted from the antenna without any information of how much is emitted at a particular frequency. It also requires the assumption for the responsivity of the bolometer. As will be discussed later below, a comparison to a blackbody source also gives an estimate of the power at each frequency.

III. RESULTS AND DISCUSSION

A. Demonstration of the operating frequency

Figure 3 shows the results for the emission spectrum of the circuit along with the background. The background is measured with the circuit off and is nonzero because the circuit is at 300 K. The interferometry technique allows the characterization of the operating frequency of the circuit. Furthermore, this technique allows us to see the operation of the fundamental and other harmonics. For a push-push oscillator scheme, it is desired that the fundamental signal is

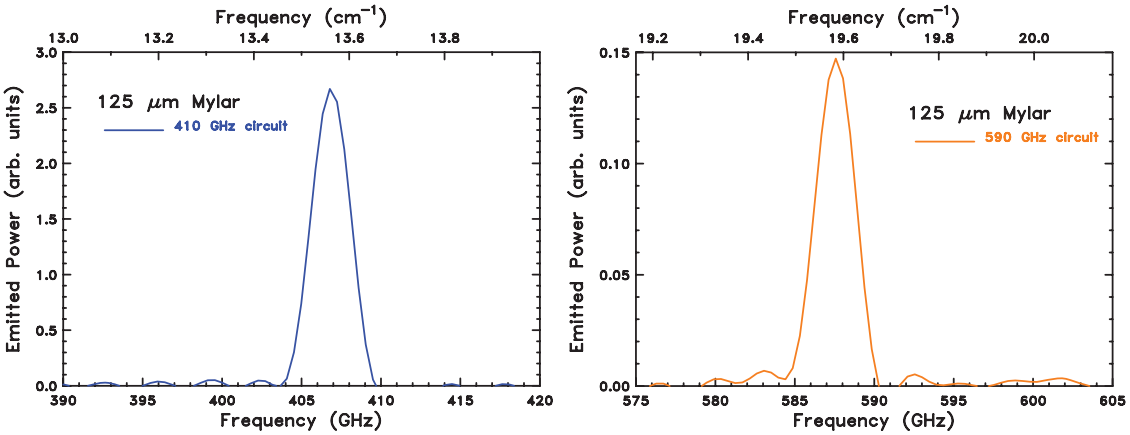

FIG. 4. (Color online) Emission spectra zoomed to the emission peaks. The results from the 125 μm beamsplitter are shown. The widths of all peaks were around 0.1 cm^{-1} (3 GHz) which correspond to the resolution limit of our interferometer. These results suggest that the true width of the circuits could not be resolved.

completely eliminated. In our previous report, the then record-breaking 410 GHz frequency was demonstrated by measuring the power from its second harmonic, but some power from the 205 GHz fundamental was also measured. (Figure 1.5, Ref. [61]). For the 410 GHz circuit presented in this paper, most of the output power is in the desired second harmonic at 410 GHz. In that respect, the circuit is an improvement over the one previously reported.[61] However, for the circuit with the fourth harmonic at 590 GHz, the second and third harmonics have higher power than that of the design frequency.

Figure 4 shows the spectrum of the circuits near the desired emission peaks (the backgrounds have been subtracted for this figure). The full width half maximum of the peak was around 0.1 cm^{-1} (3 GHz), which corresponds to the maximum resolution of our measurements and is limited by the 10 cm maximum path difference of the interferometer. The results suggest that the width of the emission peak is smaller than 0.1 cm^{-1} (3 GHz), and that we could not resolve it with our interferometry setup.

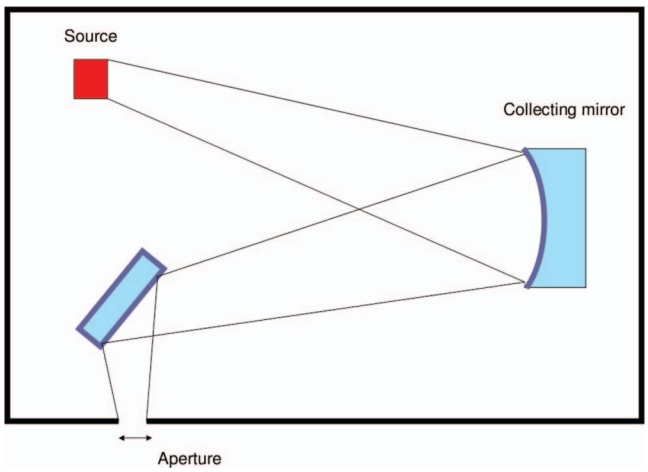

FIG. 5. (Color online) Diagram of the source compartment for the mercury lamp used in our Bruker 113 v interferometer. The collecting mirror images the source 1:1 into the aperture. The collected angle is 8.3° and the effective radiation area is that of the aperture. Not drawn to scale.

B. Estimation of the radiated power

From the absolute power measurements, placing the source next to the detector and using a lock-in amplifier, the radiation power at 410 GHz was around 100 nW. To check this result, which assumes a value of the responsivity of our bolometer, we also estimated the power from the circuit by comparing the spectra from the circuit to a blackbody source. In the Bruker 113v, or other commercially available FTIRs, the circuit can be swapped with a blackbody source easily at the source compartment, keeping the same conditions otherwise. The emission power of a blackbody source with known temperature and area can be estimated using the Rayleigh-Jeans formula for the low-frequency spectral radiance:

$$B(T) = \frac{2\upsilon^2 k_B T}{c^2}, \tag{5}$$

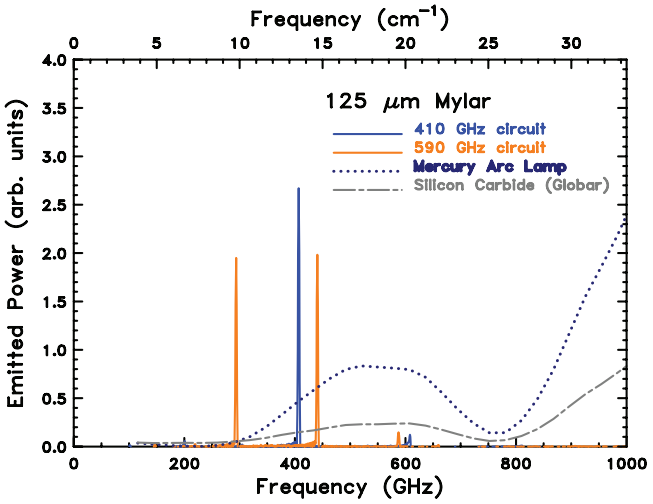

FIG. 6. (Color online) Comparison of the emission of the THz circuits (solid lines) to mercury-arc and globar lamps (dots and dashes, respectively). These are the two lamps normally used in infrared spectrometers, such as the Bruker 113v. Results for two circuits are shown, one with a second harmonic at 410 GHz (blue), and another with the fourth harmonic at 590 GHz (orange). The spectra used the 125 μm beamsplitter which has a higher signal to noise ration in the 200–600 GHz region. The emission power of the 410 GHz circuit is 5 times higher than that of the blackbody source at 14 cm^{-1}; for the other circuit, at 9 cm^{-1}, it is at least 20 times higher.

TABLE I. Power comparison between the mercury lamp and the CMOS circuits. The emission powers for the CMOS circuits were determined by comparing their spectra to that of the blackbody sources. The powers of the mercury lamp were calculated using the Rayleigh Jeans formula.

	Mercury-arc lamp	CMOS circuits
410 GHz	4.0 nW	13 nW
590 GHz	8.3 nW	1.5 nW
441 GHz	4.6 nW	15 nW
295 GHz	2.1 nW	40 nW

where $B(T)$ is the spectral radiance with SI units of W/(m^2 Hz sr), (sr refers to steradians, the units of solid angle), k_B is the Boltzmann constant equal to 1.38×10^{-23} J/K, and υ is the frequency. Our mercury-arc lamp has a temperature close to 5000 K, which yields a spectral radiance of 3×10^{-13} W/(m^2 Hz sr) at 410 GHz.

To estimate the radiation area from the blackbody source and the collected solid angle, we refer to Fig. 5. This figure shows a simple schematic of the Bruker 113v source compartment. The effective radiation area is equal to that of the aperture because the collecting mirror images the source 1:1 into the aperture (10 mm diameter). The collecting mirror has an *f*-number of $f/1.7$ and the collected angle is 8.3° with a solid angle (Ω) of 0.066 sr. Therefore, the power radiated from the mercury-arc lamp at 410 GHz, in a 3 GHz frequency bandwidth ($d\upsilon$), is approximately

$$P = B(\upsilon)\mathrm{d}\upsilon\Omega A = 4.0\ \mathrm{nW}. \quad (6)$$

The Bruker 113 v has a second source housing that allows the use of the same collecting mirror and aperture by inserting a mirror. The second source is a globar (silicon carbide) lamp with a temperature around 1500 K and an estimated power of 1.2 nW at 410 GHz. Comparison of the sources, shown in Fig. 6, suggests that the power of the 410 GHz circuit is around 13 nW. Table I shows the estimated power for all emission lines.

Another important aspect of these near-THz circuits is the high efficiency in emission per unit area. The mercury-arc lamp has an area of $\sim 8 \times 10^{-5}$ m^2, while the patch antenna of the circuits has an area in the order of 4×10^{-8} m^2 ($200\ \mu\mathrm{m} \times 200\ \mu\mathrm{m}$). This suggests that the 410 GHz source is in the order of 10 000 times brighter (emission per unit area).

IV. CONCLUSIONS

In this paper, we explain in detail how the operating frequency of a circuit in the THz region can be accurately measured using a FTIR spectrometer. Due to their small size, the circuits are highly compatible for use in a commercial FTIR. The circuits can be easily placed in the source compartment without any changes to the rest of the interferometer. This interferometry technique may be useful for future measurements of circuits pushing the frontier in operating frequency. The technique is also useful in studying a circuit with a push-push architecture, or similar architecture, designed to cancel the fundamental and use a specific harmonic. The power emitted from the circuit at different frequencies can also be directly calculated by comparison to a blackbody source. For our circuits, the value was higher than 10 nW at 410 GHz as measured by two techniques; direct power measurements using the bolometer, and comparison to a mercury-arc lamp of known temperature. Also, the relative high emission of these sources suggests that these circuits could have possible spectroscopy applications. At 410 GHz, the radiation per unit area was about 10 000 times bigger than blackbody sources. Future work in this field should consist of two goals for further use in spectroscopy. One is increasing the output power by combining multiple coupled oscillators.[64] The second is designing and building circuits with tunable frequencies. The experimental setup for interferometry described in this report is an excellent way to test and demonstrate the tunability of the circuit.

ACKNOWLEDGMENTS

This research was supported in part by the (U.S.) Department of Energy (DOE) under Grant No. DE-FG02-02ER45984 and the National Science Foundation (NSF) through NHMFL under Grant No. DMR-0520481.

[1] M. Tonouchi, Nature Photonics **1**, 97 (2007).
[2] H.-B. Liu, H. Zhong, Y. C. Nicholas Karpowicz, and X.-C. Zhang, Proc. IEEE **95**, 1514 (2007).
[3] E. Pickwell, B. E. Cole, A. J. Fitzgerald, M. Pepper, and V. P. Wallace, Phys. Med. Biol. **49**, 1595 (2004).
[4] R. Woodward, V. Wallace, D. Arnone, E. Linfield, and M. Pepper, J. Biol. Phys. **29**, 257 (2003).
[5] E. R. Mueller, *The Industrial Physicist* (American Institute of Physics, 2003), Vol. 9, issue 4, pp. 27–29.
[6] J. E. Bjarnason, T. L.J. Chan, A. W.M. Lee, M. A. Celis, and E. R. Brown, Appl. Phys. Lett. **85**, 4 (2004).
[7] J. F. Federici, B. Schulkin, F. Huang, D. Gary, R. Barat, F. Oliveira, and D. Zimdars, Semicond. Sci. Technol. **20**, S266 (2005).
[8] K. Yamamoto, M. Yamaguchi, F. Miyamaru, M. Tani, M. Hangyo, T. Ikeda, A. Matsushita, K. Koide, M. Tatsuno, and Y. Minami, Jpn. J. Appl. Phys. **43**, L414 (2004).
[9] A. Sinyukov, I. Zorych, Z.-H. Michalopoulou, D. Gary, R. Barat, and J. F. Federici, C. R. Phys. **9**, 248 (2008).
[10] R. H. Jacobsen, D. M. Mittleman, and M. C. Nuss, Opt. Lett. **24**, 2011 (1996).
[11] B. M. Fischer, H. Helm, and P. U. Jepsen, Proc. IEEE **95**, 1592 (2007).
[12] K. Kawase, Y. Ogawa, and Y. Watanabe, Opt. Express **11**, 2549 (2003).
[13] R. P. S. M. Lobo, R. L. Moreira, D. Lebeugle, and D. Colson, Phys. Rev. B **76**, 172105 (2007).
[14] T. D. Kang, E. Standard, K. H. Ahn, A. Sirenko, G. L. Carr, S. Park, Y. J. Choi, M. Ramazanoglu, V. Kiryukhin, and S. W. Cheong, Phys. Rev. B **82**, 014414 (2010).
[15] K. H. Miller, X. S. Xu, H. Berger, E. S. Knowles, D. J. Arenas, M. W. Meisel, and D. B. Tanner, Phys. Rev. B **82**, 144107 (2010).
[16] D. Talbayev, S. A. Trugman, S. Lee, H. T. Yi, S. W. Cheong, and A. J. Taylor, Phys. Rev. B **83**, 094403 (2011).
[17] T. Zhang, E. Zhukova, B. Gorshunov, D. Wu, A. S. Prokhorov, V. I. Torgashev, E. G. Maksimov, and M. Dressel, Phys. Rev. B **81**, 125312 (2010).
[18] Z. Jiang, E. A. Henriksen, L. C. Tung, Y. J. Wang, M. E. Schwartz, M. Y. Han, P. Kim, and H. L. Stormer, Phys. Rev. Lett **98**, 197403 (2007).
[19] Z. Q. Li, E. A. Henriksen, Z. Jiang, Z. Hao, M. C. Martin, P. Kim, H. L. Stormer, and D. N. Basov, Nat. Phys. **4**, 532 (2008).
[20] H. L. Liu, G. L. Carr, K. A. Worsley, M. E. Itkis, R. C. Haddon, A. N. Caruso, L. C. Tung, and Y. J. wang, New J. Phys. **12**, 113012 (2010).
[21] H. D. Drew and A. J. Sievers, Phys. Rev. Lett. **19**, 697 (1967).
[22] K. Kamarás, S. L. Herr, C. D. Porter, N. Tache, D. B. Tanner, S. Etemad, T. Venkatesan, E. Chase, A. Inam, X. D. Wu, M. S. Hegde, and B. Dutta, Phys. Rev. Lett **64**, 84 (1990).
[23] J. J. Tu, J. Li, W. Liu, A. Punnoose, Y. Gong, Y. H. Ren, L. J. Li, G. H. Cao, Z. A. Xu, and C. C. Homes, Phys. Rev. B **82**, 174509 (2010).

[24]X. Xi, J. Hwang, C. Martin, D. B. Tanner, and G. L. Carr, Phys. Rev. Lett **105**, 257006 (2010).
[25]A. D. LaForge, A. Frenzel, B. C. Pursley, T. Lin, X. Liu, J. Shi, and D. N. Basov, Phys. Rev. B **81**, 125120 (2010).
[26]P. H. Siegel, IEEE Trans. Microwave Theory Tech. **50**, 910 (2002).
[27]P. L. Richards, J. Opt. Soc. Am. **54**, 1474 (1964).
[28]R. E. Glover and M. Tinkham, Phys. Rev. **108**, 243 (1957).
[29]A. Doria, G. P. Gallerano, E. Giovenale, G. Messina, and I. Spassovsky, Phys. Rev. Lett. **93**, 264801 (2004).
[30]F. Zernike and P. R. Berman, Phys. Rev. Lett. **15**, 99 (1965).
[31]J. M. Yarborough, S. S. Sussman, H. E. Purhoff, R. H. Pantell, and B. C. Johnson, Appl. Phys. Lett. **15**, 102 (1969).
[32]K. H. Yang, P. L. Richards, and Y. R. Shen, Appl. Phys. Lett. **19**, 320 (1971).
[33]K. Kawase, M. Sato, T. Taniuchi, and H. Ito, Appl. Phys. Lett. **68**, 2483 (1996).
[34]S. Hayashi, T. Shibuya, H. Sakai, T. Taira, C. Otani, Y. Ogawa, and K. Kawase, Appl. Opt. **48**, 2899 (2009).
[35]D. H. Auston, K. P. Cheung, and P. R. Smith, Appl. Phys. Lett. **45**, 284 (1984).
[36]C. Fattinger and D. Grischkowsky, Appl. Phys. Lett. **54**, 490 (1989).
[37]X. C. Zhang, B. B. Hu, J. T. Darrow, and D. H. Auston, Appl. Phys. Lett. **56**, 1011 (1990).
[38]L. Xu, X. C. Zhang, B. Jalali, and D. H. Auston, Appl. Phys. Lett. **59**, 3357 (1991).
[39]D. You, R. R. Jones, P. H. Bucksbaum, and D. R. Dykaar, Opt. Lett. **18**, 290 (1993).
[40]S. Matsuura, G. A. Blake, R. A. Wyss, J. C. Pearson, C. Kadow, A. W. Jackson, and A. C. Gossard, Appl. Phys. Lett. **74**, 2872 (1999).
[41]D. H. Auston, K. P. Cheung, J. A. VAldmanis, and D. A. Kleinman, Phys. Rev. Lett. **53**, 1555 (1984).
[42]L. Xu, X. C. Zhang, and D. H. Auston, Appl. Phys. Lett. **61**, 1784 (1992).
[43]D. Grischkowsky, S. Keiding, M. V. Exter, and C. Fattinger, J. Opt. Soc. Am. B **7**, 2006 (1990).
[44]M. V. Exter, C. Fattinger, and D. Grischkowsky, Opt. Lett. **14**, 1128 (1989).
[45]S. Kono, M. Tani, P. Gu, and K. Sakai, Appl. Phys. Lett. **77**, 4104 (2000).
[46]Q. Wu and X. C. Zhang, Appl. Phys. Lett. **67**, 3523 (1995).
[47]P. Y. Han, M. Tani, M. Usami, S. Kono, R. Kersting, and X. C. Zhang, J. Appl. Phys. **89**, 2357 (2001).
[48]B. Xu, X. Hu, and M. R. Melloch, Appl. Phys. Lett. **71**, 440 (1997).
[49]R. Kohler, H. A. Tredicucci, F. Beltram, H. E. Beere, E. H. Linfield, A. G. Davies, D. A. Ritchie, R. C. Iotti, and F. Rossi, Nature (London) **417**, 156 (2002).
[50]B. S. Williams, Nature Photonics **1**, 517 (2007).
[51]G. Scalari, C. Walther, M. Fischer, R. Terazzi, H. Beere, D. Ritchie, and J. Faist, Laser Photonics Rev. **3**, 1 (2009).
[52]C. Walther, M. Fischer, G. Scalari, R. Terazzi, N. Hoyler, and J. Faist, Appl. Phys. Lett. **91**, 131122 (2007).
[53]S. Kumar, Q. Hu, and J. L. Reno, Appl. Phys. Lett. **94**, 131105 (2009).
[54]S. Kumar, C. W. Chan, Q. Hu, and J. L. Reno, Nat. Phys. **7**, 167 (2011).
[55]J. M. Byrd, W. P. Leemans, A. Loftsdottir, B. Marcelis, M. C. Martin, W. R. McKinney, F. Sannibale, T. Scarvie, and C. Steier, Phys. Rev. Lett. **89**, 224801 (2002).
[56]M. Abo-Bakr, J. Feikes, K. Holldack, G. Wstefeld, and H. W. Hbers, Phys. Rev. Lett. **88**, 254801 (2002).
[57]G. L. Carr, M. C. Martin, W. R. McKinne, K. Jordan, G. R. Neil, and G. P. Williams, Nature (London) **420**, 153 (2002).
[58]W. P. Leemans, C. G.R. Geddes, J. Faure, C. S. Toth, J. V. Tilborg, C. B. Schroeder, E. Esarey, G. Fubiani, D. Auerbach, B. Marcelis, M. A. Carnahan, R. A. Kaindl, J. Byrd, and M. C. Martin, Phys. Rev Lett. **91**, 074802 (2003).
[59]S. E. Korbly, A. S. Kesar, J. R. Sirigiri, and R. J. Temkin, Phys. Rev. Lett. **94**, 054803 (2005).
[60]S. Sankaran, E. Seok, C. Cao, R. Han, D. Shim, S. H. Hill, D. J. Arenas, D. B. Tanner, C. Hung, and K. O, *Solid-State Circuits Conference - Digest of Technical Papers, 2009. ISSCC 2009. IEEE International*, pp. 202–203, 203a, 8–12 Feb. 2009.
[61]E. Seok, C. Cao, D. Shim, D. J. Arenas, D. B. Tanner, C. Hung, and K. O, *Solid-State Circuits Conference, 2008. ISSCC 2008, Digest of Technical Papers, IEEE International*, pp. 472–629, 3–7 Feb. 2008.
[62]E. Seok, D. Shim, D. J. Arenas, D. B. Tanner, and K. K. O, IEEE Microw. Wirel. Compon. Lett. **20**, 554 (2010).
[63]E. Seok, Ph.D. dissertation, University of Florida, 2009.
[64]R. A. York, IEEE Trans. Microwave **39**, 1000 (1991).